WALAILAK JOURNAL
http://wjst.wu.ac.th Mathematics

# Analytical Solution for Three-Dimensional Steady Flow of Condensation Film on Inclined Rotating Disk by Optimal Homotopy Analysis Method

**Hany Nasr HASSAN[1,*] and Mohammad Mehdi RASHIDI[2]**

[1]*Department of Basic Science, Faculty of Engineering, Benha University, Benha, Egypt*
[2]*Faculty of Engineering, Bu-Ali Sina University, Hamedan, Iran*

**([*]Corresponding author's e-mail: h_nasr77@yahoo.com)**

*Received: 1 February 2012, Revised: 24 July 2012, Accepted: 25 June 2013*

**Abstract**

In this paper, the Optimal Homotopy Analysis Method (OHAM) has been used to derive a highly accurate analytic solution for the steady three-dimensional problem of a condensation film on an inclined rotating disk. With a similarity solution method, the governing equations can be reduced to a system of nonlinear ordinary differential equations (ODEs). The control parameter (ħ) in the HAM is derived by using the averaged residual error method. Using the optimal control parameter provides a superior control on the convergence and accuracy of the analytical solution. The velocity and temperature profiles are shown and the influence of Prandtl number on the temperature profiles is discussed in detail. The validity of the obtained solutions is verified by the numerical results.

**Keywords:** Homotopy analysis method, optimal convergence-control parameter, series solution, rotating disk, film thickness

## Introduction

Most phenomena in our world are essentially nonlinear and are described by nonlinear equations. Some of them are solved using numerical methods and some are solved using the analytical methods of perturbation [1,2]. The numerical methods give the solution at discrete points and thus it is often costly and time consuming to get a complete curve of results and furthermore, stability and convergence should be considered so as to avoid divergence or inappropriate results. In the perturbation methods, one should exert the small parameter in the governing equation. Therefore, finding the small parameter and inserting it into the equation are deficiencies of perturbation methods. One semi-exact method which does not need a small/large parameter is the Homotopy Analysis Method (HAM), first proposed by Liao in 1992 [3]. Liao employed the basic ideas of the homotopy in topology to propose a general analytical method for nonlinear problems, namely the homotopy analysis method. The HAM can overcome the foregoing restrictions and limitations of perturbation methods [4]. The HAM also avoids discretization and provides an efficient solution with high accuracy, minimal calculation and avoidance of physically unrealistic assumptions. More importantly, unlike the perturbation and non-perturbation methods, the HAM provides a simple way to ensure the convergence of series solutions so that one can always get accurate enough approximations even for strongly nonlinear problems. Furthermore, the HAM provides the freedom to choose the so-called auxiliary linear operator so that one can approximate a nonlinear problem more effectively by means of better base functions [5]. The HAM has already been successfully applied to solve many types of nonlinear problems such as the flows of non-Newtonian fluids over a stretching sheet [6,7], unsteady three dimensional flows [8], Jaulent-Miodek equations [9], Burgers and regularized long wave equations [10], two-dimensional viscous flow in a rectangular domain bounded by two moving

porous walls [11], the nonlinear equations arising in heat transfer [12], two-point nonlinear boundary value problems [13], a new technique of using homotopy analysis method for solving high-order nonlinear differential equations [14], prediction of multiplicity of solutions of nonlinear boundary value problems [15], Schrödinger equations [16], simultaneous effects of partial slip and thermal-diffusion and diffusion-thermo on steady magnetohydrodynamic (MHD) convective flow due to a rotating disk [17], analytical solution for off-centered stagnation flow towards a rotating disc problem by the homotopy analysis method with two control parameters [18] and many other problems. Removing a condensate liquid from a cooled, saturated vapor is important in engineering processes. Sparrow and Gregg [19] considered the removal of the condensate using centrifugal forces on a cooled rotating disk. Following von Karman's [20] study of a rotating disk in an infinite fluid, Sparrow and Gregg transformed the Navier-Stokes equations into a set of nonlinear ordinary differential equations and numerically integrated for the similarity solution for several finite film thicknesses. Their work was extended by adding vapor drag by Beckett *et al.* [21] and adding suction on the plate by Chary and Sarma [22]. The problem is also related to chemical vapor deposition, when a thin fluid film is deposited on a cooled rotating disk [23]. In this paper, the HAM is applied to find the totally analytical solution for the problem of condensation or spraying on an inclined rotating disk and the obtained solution is compared with the numerical solution. This problem was studied first by Wang [24], and Rashidi *et al.* [25] who applied the DTM for it; please also see [26,27].

**Flow analysis and mathematical formulation**

**Figure 1** shows a disk rotating in its own plane with angular velocity $\Omega$. The angle between the horizontal axis and disk is $\beta$. A fluid film of thickness $t$ is formed by spraying, with a velocity $W$. We assume the disk radius is large compared to the film thickness such that the end effects can be ignored. Vapor shear effects at the interface of vapor and fluid are usually also unimportant. The gravitational acceleration, $\overline{g}$ acts in the downward direction. The temperature on the disk is $T_w$ and the temperature on the film surface is $T_0$. Besides, the ambient pressure on the film surface is constant at $p_0$ and we can safely say the pressure is a function of $z$ only. Neglecting viscous dissipation, the continuity, momentum and energy equations for the steady state are given in the following form;

$$u_x + v_y + w_z = 0, \tag{1}$$

$$u u_x + v u_y + w u_z = \nu\left(u_{xx} + u_{yy} + u_{zz}\right) + \overline{g}\sin\beta, \tag{2}$$

$$u v_x + v v_y + w v_z = \nu\left(v_{xx} + v_{yy} + v_{zz}\right), \tag{3}$$

$$u w_x + v w_y + w w_z = \nu\left(w_{xx} + w_{yy} + w_{zz}\right) - \overline{g}\cos\beta - p_z/\rho, \tag{4}$$

$$u T_x + v T_y + w T_z = \alpha\left(T_{xx} + T_{yy} + T_{zz}\right). \tag{5}$$

In the above equations, $u$, $v$, and $w$ indicate the velocity components in the $x$, $y$, and z directions, respectively; $T$ denotes the temperature, $\rho$, $\nu$ and $\alpha$ are the density, kinematic viscosity and thermal diffusivity of the fluid, respectively. Supposing zero slip on the disk and zero shear stress on the film surface, the boundary conditions are;

$$\begin{aligned} &u = -\Omega y, \quad v = \Omega x, \quad w = 0, \quad T = T_w \quad \text{at } z = 0, \\ &u_z = 0, \quad v_z = 0, \quad w = -W, \quad T = T_0, \quad p = p_0 \quad \text{at } z = t. \end{aligned} \tag{6}$$

For the mentioned problem, Wang introduced the following transformation [24];

$$u = -\Omega\, y\, g(\eta) + \Omega\, x\, f'(\Omega) + \overline{g}\, k(\eta) \sin\frac{\beta}{\Omega},$$

$$v = \Omega\, x\, g(\eta) + \Omega\, y\, f'(\Omega) + \overline{g}\, s(\eta) \sin\frac{\beta}{\Omega}, \tag{7}$$

$$w = -2\sqrt{\Omega v}\, f(\eta), \qquad T = \left(T_0 - T_w\right)\theta(\eta) + T_w,$$

where $\eta = z\sqrt{\Omega / v}$. (8)

Continuity in Eq. (1) is automatically satisfied. Eqs. (2) and (3) can be written as follows;

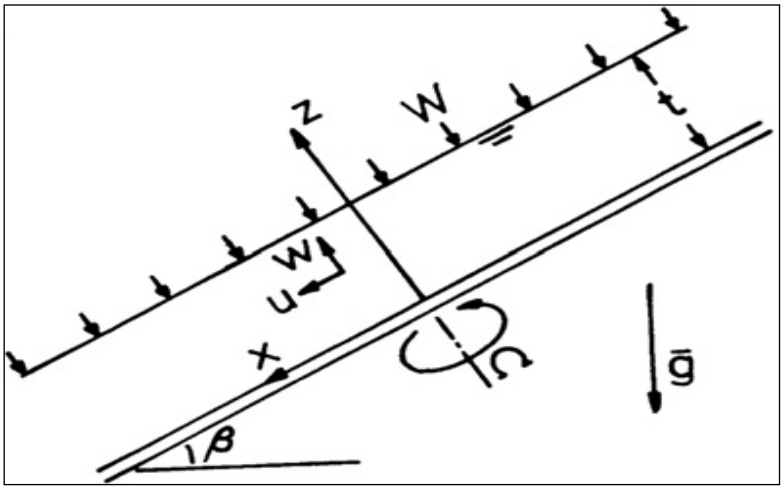


**Figure 1** Schematic diagram of the problem.

$$f''' - \left(f'\right)^2 + g^2 + 2f\, f'' = 0, \tag{9}$$

$$g'' - 2g\, f' + 2f\, g' = 0, \tag{10}$$

$$k'' - k\, f' + s\, g + 2f\, k' + 1 = 0, \tag{11}$$

$$s'' - g\, k - s\, f' + 2f\, s' = 0. \tag{12}$$

If the temperature is a function of the distance $z$ only, Eq. (5) becomes;

$$\theta'' + 2\,\mathrm{Pr}\, f\theta' = 0, \tag{13}$$

where $\mathrm{Pr} = v/\alpha$ is the Prandtl number and $f$, $g$, $k$, $s$ and $\theta$ nondimentional functions in $\eta$ [25]. The boundary conditions for Eqs. (9) - (13) are;

$$f(0) = 0, \quad f'(0) = 0, \quad f''(\delta) = 0, \quad g(0) = 1, \quad g'(\delta) = 0, \quad k(0) = 0, \quad k'(\delta) = 0,$$
$$s(0) = 0, \quad s'(\delta) = 0, \quad \theta(0) = 0, \quad \theta(\delta) = 1, \tag{14}$$

and $\delta$ is the constant normalized thickness as;

$$\delta = t\sqrt{\Omega / \nu}\ . \tag{15}$$

After the flow field is found, the pressure can be obtained by integrating Eq. (4);

$$p(z) = p_0 + \rho\Big[\nu\big[w_z(z) - w_z(t)\big] - \Big[w^2(z) - w^2(t)\Big]/2 - \overline{g}(z-t)\cos\beta\Big]. \tag{16}$$

**Analytical approximation solutions with the HAM**

The basic idea of the HAM, as described in detail by Liao [28], according to the boundary conditions (14) and the rules of the solution expression, we choose;

$$f_0(\eta) = \frac{1}{3}\left(3\delta\eta^2 - \eta^3\right),\quad g_0(\eta) = 1,\quad k_0(\eta) = \frac{1}{2}\left(2\delta\eta - \eta^2\right),$$
$$s_0(\eta) = \frac{1}{2}\left(2\delta\eta - \eta^2\right),\quad \theta_0(\eta) = \frac{\eta}{\delta}, \tag{17}$$

as the initial guesses of $f(\eta)$, $g(\eta)$, $k(\eta)$, $s(\eta)$ and $\theta(\eta)$, satisfying the boundary conditions (14). The auxiliary linear operators $L_1, L_2, L_3, L_4$ and $L_5$ are;

$$L_1(f) = \frac{\partial^3 f}{\partial\eta^3},\ L_2(g) = \frac{\partial^2 g}{\partial\eta^2},\quad L_3(k) = \frac{\partial^2 k}{\partial\eta^2},\ L_4(s) = \frac{\partial^2 s}{\partial\eta^2},\ L_5(\theta) = \frac{\partial^2\theta}{\partial\eta^2}, \tag{18}$$

which satisfy the following properties;

$$L_1(c_1 + c_2\eta + c_3\eta^2) = 0,\ L_2(c_4 + c_5\eta) = 0,\ L_3(c_6 + c_7\eta) = 0,$$
$$L_4(c_8 + c_9\eta) = 0,\quad L_5(c_{10} + c_{11}\eta) = 0\ . \tag{19}$$

where $c_i$, $i = 1, 2, \ldots, 11$ are arbitrary constants. Let $q \in [0,1]$ denotes an embedding parameter, $\hbar_1$, $\hbar_2$ and $\hbar_3$ are control nonzero parameters. Then the zeroth-order deformation equations are of the following form;

$$(1-q)\,L_1\Big[\hat{f}(\eta;q) - f_0(\eta)\Big] = q\,\hbar_1 N_1\Big[\hat{f}(\eta;q),\ \hat{g}(\eta,q)\Big], \tag{20}$$
$$(1-q)\,L_2\big[\hat{g}(\eta,q) - g_0(\eta)\big] = q\,\hbar_1 N_2\Big[\hat{f}(\eta;q),\ \hat{g}(\eta,q)\Big], \tag{21}$$
$$(1-q)\,L_3\Big[\hat{k}(\eta,q) - k_0(\eta)\Big] = q\,\hbar_2 N_3\Big[\hat{f}(\eta;q),\ \hat{g}(\eta,q),\ \hat{k}(\eta,q),\ \hat{s}(\eta,q)\Big], \tag{22}$$
$$(1-q)\,L_4\big[\hat{s}(\eta,q) - s_0(\eta)\big] = q\,\hbar_2 N_4\Big[\hat{f}(\eta;q),\ \hat{g}(\eta,q),\ \hat{k}(\eta,q),\ \hat{s}(\eta,q)\Big], \tag{23}$$
$$(1-q)\,L_5\Big[\hat{\theta}(\eta;q) - \theta_0(\eta)\Big] = q\,\hbar_3 N_5\Big[\hat{f}(\eta;q),\ \hat{\theta}(\eta,q)\Big], \tag{24}$$

Subject to the boundary conditions;

$$\hat{f}(0;q)=0,\quad \hat{f}'(0;q)=0,\quad \hat{f}''(\delta;q)=0,\quad \hat{g}(0;q)=1,\quad \hat{g}'(\delta;q)=0,\quad \hat{k}(0;q)=0,$$
$$\hat{k}'(\delta;q)=0,\quad \hat{s}(0;q)=0,\quad \hat{s}'(\delta;q)=0,\quad \hat{\theta}(0;q)=0,\quad \hat{\theta}(\delta;q)=1. \tag{25}$$

In which we define the nonlinear operators $N_1, N_2, N_3, N_4$ and $N_5$ as;

$$N_1=\frac{\partial^3\hat{f}(\eta;q)}{\partial\eta^3}-\left(\frac{\partial\hat{f}(\eta;q)}{\partial\eta}\right)^2+\left(\hat{g}(\eta;q)\right)^2+2\hat{f}(\eta;q)\frac{\partial^2\hat{f}(\eta;q)}{\partial\eta^2}, \tag{26}$$

$$N_2=\frac{\partial^2\hat{g}(\eta;q)}{\partial\eta^2}-2\hat{g}(\eta;q)\frac{\partial\hat{f}(\eta;q)}{\partial\eta}+2\hat{f}(\eta;q)\frac{\partial\hat{g}(\eta;q)}{\partial\eta}, \tag{27}$$

$$N_3=\frac{\partial^2\hat{k}(\eta;q)}{\partial\eta^2}-\hat{k}(\eta;q)\frac{\partial\hat{f}(\eta;q)}{\partial\eta}+\hat{s}(\eta;q)\,\hat{g}(\eta;q)+2\hat{f}(\eta;q)\frac{\partial\hat{k}(\eta;q)}{\partial\eta}+1, \tag{28}$$

$$N_4=\frac{\partial^2\hat{s}(\eta;q)}{\partial\eta^2}-\hat{k}(\eta;q)\hat{g}(\eta;q)-\hat{s}(\eta;q)\frac{\partial\hat{f}(\eta;q)}{\partial\eta}+2\hat{f}(\eta;q)\frac{\partial\hat{s}(\eta;q)}{\partial\eta}, \tag{29}$$

$$N_5=\frac{\partial^2\hat{\theta}(\eta;q)}{\partial\eta^2}+2\,\mathrm{Pr}\,\hat{f}(\eta;q)\frac{\partial\hat{\theta}(\eta;q)}{\partial\eta}. \tag{30}$$

Clearly, when $q = 0$ the zero-order deformation Eqs. (20) - (24) give rise to;

$$\hat{f}(\eta;0)=f_0(\eta),\quad \hat{g}(\eta;0)=g_0(\eta),\quad \hat{k}(\eta;0)=k_0(\eta),\quad \hat{s}(\eta;0)=s_0(\eta),\quad \hat{\theta}(\eta;0)=\theta_0(\eta). \tag{31}$$

when $q = 1$, they become;

$$\hat{f}(\eta;1)=f(\eta),\quad \hat{g}(\eta;1)=g(\eta),\quad \hat{k}(\eta;1)=k(\eta),\quad \hat{s}(\eta;1)=s(\eta),\quad \hat{\theta}(\eta;1)=\theta(\eta). \tag{32}$$

Expanding $\hat{f}(\eta), \hat{g}(\eta), \hat{k}(\eta), \hat{s}(\eta)$ and $\hat{\theta}(\eta)$ in a Maclaurin series with respect to the embedding parameter $q$, we obtain;

$$\hat{f}(\eta;q)=f_0(\eta)+\sum_{m=1}^{+\infty}f_m(\eta)\,q^m,\quad \hat{g}(\eta;q)=g_0(\eta)+\sum_{m=1}^{+\infty}g_m(\eta)\,q^m,$$
$$\hat{k}(\eta;q)=k_0(\eta)+\sum_{m=1}^{+\infty}k_m(\eta)\,q^m,$$
$$\hat{s}(\eta;q)=s_0(\eta)+\sum_{m=1}^{+\infty}s_m(\eta)\,q^m,\quad \hat{\theta}(\eta;q)=\theta_0(\eta)+\sum_{m=1}^{+\infty}\theta_m(\eta)\,q^m, \tag{33}$$

where

$$f_m(\eta)=\frac{1}{m!}\frac{\partial^m \hat{f}(\eta;q)}{\partial q^m}\bigg|_{q=0},\ g_m(\eta)=\frac{1}{m!}\frac{\partial^m \hat{g}(\eta;q)}{\partial q^m}\bigg|_{q=0},\ k_m(\eta)=\frac{1}{m!}\frac{\partial^m \hat{k}(\eta;q)}{\partial q^m}\bigg|_{q=0},$$
$$s_m(\eta)=\frac{1}{m!}\frac{\partial^m \hat{s}(\eta;q)}{\partial q^m}\bigg|_{q=0},\ \theta_m(\eta)=\frac{1}{m!}\frac{\partial^m \hat{\theta}(\eta;q)}{\partial q^m}\bigg|_{q=0}, \tag{34}$$

The convergence of the series (33) strongly depends upon the control parameters $\hbar_1$, $\hbar_2$ and $\hbar_3$. Assuming that $\hbar_1$, $\hbar_2$ and $\hbar_3$ are selected such that the series (33) are convergent at $q = 1$ then due to Eqs. (31) and (32) we have;

$$f(\eta)=f_0(\eta)+\sum_{m=1}^{+\infty} f_m(\eta),\quad g(\eta)=g_0(\eta)+\sum_{m=1}^{+\infty} g_m(\eta),\quad k(\eta)=k_0(\eta)+\sum_{m=1}^{+\infty} k_m(\eta),$$
$$s(\eta)=s_0(\eta)+\sum_{m=1}^{+\infty} s_m(\eta),\quad \theta(\eta)=\theta_0(\eta)+\sum_{m=1}^{+\infty} \theta_m(\eta), \tag{35}$$

Differentiating the zero-order deformation Eqs. (20) - (24) $m$ times with respect to $q$, then setting $q = 0$ and finally dividing by $m!$, we have the $m$th-order deformation equations;

$$L_1\left[f_m-\chi_m f_{m-1}\right]=\hbar_1 R_{1,m},\quad L_2\left[g_m-\chi_m g_{m-1}\right]=\hbar_1 R_{2,m},\quad L_3\left[k_m-\chi_m k_{m-1}\right]=\hbar_2 R_{3,m},$$
$$L_4\left[s_m-\chi_m s_{m-1}\right]=\hbar_2 R_{4,m},\quad L_5\left[\theta_m-\chi_m \theta_{m-1}\right]=\hbar_3 R_{5,m}. \tag{36}$$

With the following boundary conditions;

$$f_m(0)=0,\ f_m'(0)=0,\ f_m''(\delta)=0,\ g_m(0)=0,\ g_m'(\delta)=0,\ k_m(0)=0,\ k_m'(\delta)=0,$$
$$s_m(0)=0,\ s_m'(\delta)=0,\ \theta_m(0)=0,\ \theta_m(\delta)=0, \tag{37}$$

where

$$R_{1,m}=\frac{1}{(m-1)!}\frac{\partial^{m-1}N_1}{\partial q^{m-1}}\bigg|_{q=0}=\frac{\partial^3 f_{m-1}}{\partial\eta^3}+\sum_{i=0}^{m-1}\left(-\frac{\partial f_{m-1}}{\partial\eta}\frac{\partial f_{m-1-i}}{\partial\eta}+g_i\, g_{m-1-i}+2f_i\frac{\partial^2 f_{m-1-i}}{\partial\eta^2}\right), \tag{38}$$

$$R_{2,m}=\frac{1}{(m-1)!}\frac{\partial^{m-1}N_2}{\partial q^{m-1}}\bigg|_{q=0}=\frac{\partial^2 g_{m-1}}{\partial\eta^2}+\sum_{i=0}^{m-1}\left(-2g_i\frac{\partial f_{m-1-i}}{\partial\eta}+2f_i\frac{\partial g_{m-1-i}}{\partial\eta}\right), \tag{39}$$

$$R_{3,m}=\frac{1}{(m-1)!}\frac{\partial^{m-1}N_3}{\partial q^{m-1}}\bigg|_{q=0}=\frac{\partial^2 k_{m-1}}{\partial\eta^2}+\sum_{i=0}^{m-1}\left(-k_i\frac{\partial f_{m-1-i}}{\partial\eta}+s_i g_{m-1-i}+2f_i\frac{\partial k_{m-1-i}}{\partial\eta}\right)+(1-\chi_m), \tag{40}$$

$$R_{4,m}=\frac{1}{(m-1)!}\frac{\partial^{m-1}N_4}{\partial q^{m-1}}\bigg|_{q=0}=\frac{\partial^2 s_{m-1}}{\partial\eta^2}+\sum_{i=0}^{m-1}\left(-k_i g_{m-1-i}-s_i\frac{\partial f_{m-1-i}}{\partial\eta}+2f_i\frac{\partial s_{m-1-i}}{\partial\eta}\right), \tag{41}$$

$$R_{5,m} = \frac{1}{(m-1)!}\frac{\partial^{m-1} N_5}{\partial q^{m-1}}\bigg|_{q=0} = \frac{\partial^2 \theta_{m-1}}{\partial \eta^2} + \Pr \sum_{i=0}^{m-1}\left(2 f_i \frac{\partial \theta_{m-1-i}}{\partial \eta}\right), \tag{42}$$

and $$\chi_m = \begin{cases} 0, & m \le 1, \\ 1, & m > 1. \end{cases} \tag{43}$$

Then the solutions for Eq. (36) can be expressed by;

$$f_m(\eta) = \chi_m f_{m-1} + \hbar_1 L_1^{-1}\left[R_{1,m}\right] + c_1 + c_2\,\eta + c_3\,\eta^2, \tag{44}$$

$$g_m(\eta) = \chi_m g_{m-1} + \hbar_1 L_2^{-1}\left[R_{2,m}\right] + c_4 + c_5\,\eta, \tag{45}$$

$$k_m(\eta) = \chi_m\, k_{m-1} + \hbar_2 L_3^{-1}\left[R_{3,m}\right] + c_6 + c_7\,\eta, \tag{46}$$

$$s_m(\eta) = \chi_m s_{m-1} + \hbar_2 L_4^{-1}\left[R_{4,m}\right] + c_8 + c_9\,\eta, \tag{47}$$

$$\theta_m(\eta) = \chi_m\, \theta_{m-1} + \hbar_3 L_5^{-1}\left[R_{5,m}\right] + c_{10} + c_{11}\,\eta, \tag{48}$$

where $c_i$, $i = 1, 2, \ldots, 11$ are constants to be determined by the boundary conditions (37), $L_1^{-1}, L_2^{-1}$, $L_3^{-1}, L_4^{-1}$ and $L_5^{-1}$ denote the inverse linear operators of $L_1$, $L_2$, $L_3$, $L_4$ and $L_5$ respectively. For example, we can obtain the following results for solving the first order deformation equation;

$$f_1(\eta) = \frac{\hbar_1}{360}\left(-105\,\eta^3 + \eta^7 + 315\,\eta^2\,\delta - 7\,\eta^6\,\delta + 84\,\eta^2\,\delta^5\right), \tag{49}$$

$$g_1(\eta) = \frac{\hbar_1}{6}\left(\eta^4 - 4\,\eta^3\,\delta + 8\,\eta\,\delta^3\right), \tag{50}$$

$$k_1(\eta) = \frac{\hbar_2}{360}\left(-15\,\eta^4 + 2\eta^6 + 60\,\eta^3\,\delta - 12\,\eta^5\,\delta - 120\,\eta\,\delta^3 + 48\,\eta\,\delta^5\right), \tag{51}$$

$$s_1(\eta) = \frac{\hbar_2}{360}\left(-180\,\eta^2 + 15\eta^4 + 2\,\eta^6 + 360\,\eta\,\delta - 60\eta^3\,\delta - 12\eta^5\,\delta + 120\eta\,\delta^3 + 48\eta\,\delta^5\right), \tag{52}$$

$$\theta_1(\eta) = \frac{\Pr\hbar_3}{30\,\delta}\left(-\eta^5 + 5\,\eta^4\,\delta - 4\,\eta\,\delta^4\right), \tag{53}$$

$f_m(\eta)$, $g_m(\eta)$, $k_m(\eta)$, $s_m(\eta)$ and $\theta_m(\eta)$ for $m$ = 2, 3,…, can be calculated similarly with the aid of mathematical software such as Mathematica or Maple. At the $M$th- order approximation, we have the analytic solution of (9) - (14), namely;

$$f(\eta) \approx \sum_{m=0}^{M} f_m(\eta), \quad g(\eta) \approx \sum_{m=0}^{M} g_m(\eta), \quad k(\eta) \approx \sum_{m=0}^{M} k_m(\eta),$$
$$s(\eta) \approx \sum_{m=0}^{M} s_m(\eta), \quad \theta(\eta) \approx \sum_{m=0}^{M} \theta_m(\eta), \tag{54}$$

**Convergence of the HAM solutions**

The series solutions of the functions $f_m(\eta)$, $g_m(\eta)$, $k_m(\eta)$, $s_m(\eta)$ and $\theta_m(\eta)$ are given in Eq. (35). The convergence of these series and rate of the approximation for the HAM strongly depend upon the values of the convergence control parameters, $\hbar_1$, $\hbar_2$ and $\hbar_3$. In the usual HAM [28], there is only one unknown convergence-control parameter, $\hbar$. In order to obtain the admissible value of $\hbar$ for the present problem, $\hbar_1 = \hbar_2 = \hbar_3 = \hbar$ is assumed and the $\hbar$-curves are plotted for 10th-order approximations. One can determine the possible valid region of $\hbar$ as shown in **Figures 2 - 6**, but unfortunately it cannot tell us which value of $\hbar$ gives the fastest convergent series. However, in the expression of the obtained solution, there are 3 unknown convergence control parameters, $\hbar_1$, $\hbar_2$ and $\hbar_3$, which not only can make sure the convergence of the solutions, but also can give the fastest convergent series by using the possible optimal values of convergence-control parameters determined by minimizing the averaged residual error [29];

$$E_{j,M} = \frac{1}{K}\sum_{i=1}^{K}\left[ N_j\left(\sum_{i=1}^{M} f(i\Delta\eta), \sum_{i=1}^{M} g(i\Delta\eta), \sum_{i=1}^{M} k(i\Delta\eta), \sum_{i=1}^{M} s(i\Delta\eta), \sum_{i=1}^{M} \theta(i\Delta\eta)\right)\right]^2, \quad j = 1,2,3. \tag{55}$$

Corresponding to the nonlinear algebraic equations;

$$\frac{\partial E_{j,M}}{\partial \hbar_1} = 0, \quad \frac{\partial E_{j,M}}{\partial \hbar_2} = 0, \quad \frac{\partial E_{j,M}}{\partial \hbar_3} = 0. \tag{56}$$

Using the symbolic computation software Mathematica, by minimizing the averaged residual error Eq. (55), the optimal convergence-control parameters can be obtained directly at 10th-order approximation, where $\Delta\eta = \delta / K$ and $K = 20$ in this problem. The optimal values of $\hbar_1$ and $\hbar_2$ for different values of $\delta$ at 10th-order approximation are presented **Table 1**, and the optimal value of $\hbar_3$ for different values of $\delta$ and Pr at 10th-order approximation are shown in **Table 2**. To see the accuracy of the solutions, substituting the approximate solution of $f(\eta)$, $g(\eta)$, $k(\eta)$, $s(\eta)$ and $\theta(\eta)$ obtained by the 10th-order approximation yields the residual error as follows;

$$\mathrm{Res}\, f = f''' - (f')^2 + g^2 + 2ff'', \tag{57}$$
$$\mathrm{Res}\, g = g'' - 2gf' + 2fg', \tag{58}$$
$$\mathrm{Res}\, k = k'' - kf' + sg + 2fk' + 1, \tag{59}$$
$$\mathrm{Res}\, s = s - gk - sf' + 2fs', \tag{60}$$
$$\mathrm{Res}\, \theta = \theta'' + 2\,\mathrm{Pr}\,\theta'. \tag{61}$$

If Res = 0 then the approximate solution obtained by the HAM happens to be the exact solution. Generally, such a situation does not arise for nonlinear problems. Residual errors of $f(\eta)$, $g(\eta)$, $k(\eta)$, $s(\eta)$ and $\theta(\eta)$ obtained by the 10th-order approximation for δ = 0.5 and δ = 1 at Pr = 20 are presented in **Figures 7 - 16**.

**Results and discussion**

In order to verify the accuracy of the used method, the HAM results of $f(\eta), g(\eta)$, $k(\eta)$ and $s(\eta)$ compared with the numerical solutions obtained by the fifth-order Runge-Kutta method in **Table 3**. One can see a good agreement between the analytical results of the HAM and numerical results as shown in **Tables 3** and **4** and shown in **Figures 17** and **18**. The normalized temperature profiles for different values of the Prandtl number are represented in **Figures 19** and **20** at δ = 0.5 and δ = 1, respectively. The Prandtl number ranges from 0.1 for liquid metals, to 7 for water and to more than 100 for some oils. In **Figures 19** and **20** and **Table 2**, it can be seen that the HAM solution contains all groups.

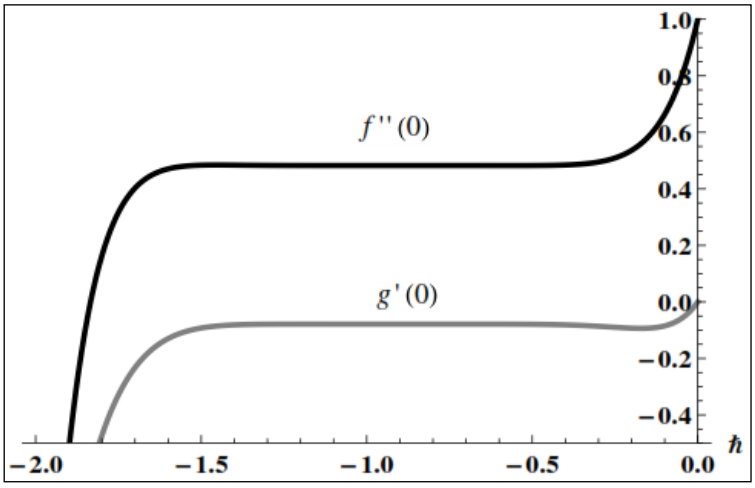


**Figure 2** The ħ-curves of $f''(0)$ and $g'(0)$ obtained by the 10th order approximation of HAM, when $\delta = 0.5$.

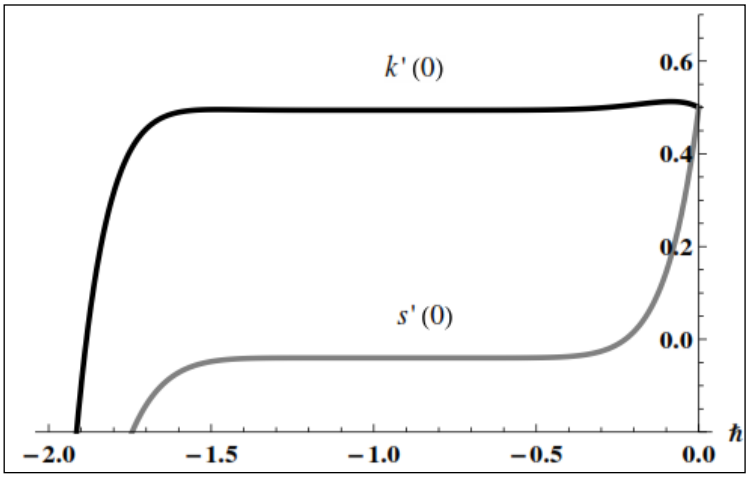


**Figure 3** The ħ-curves of $k'(0)$ and $s'(0)$ obtained by the 10th order approximation of HAM, when $\delta = 0.5$.

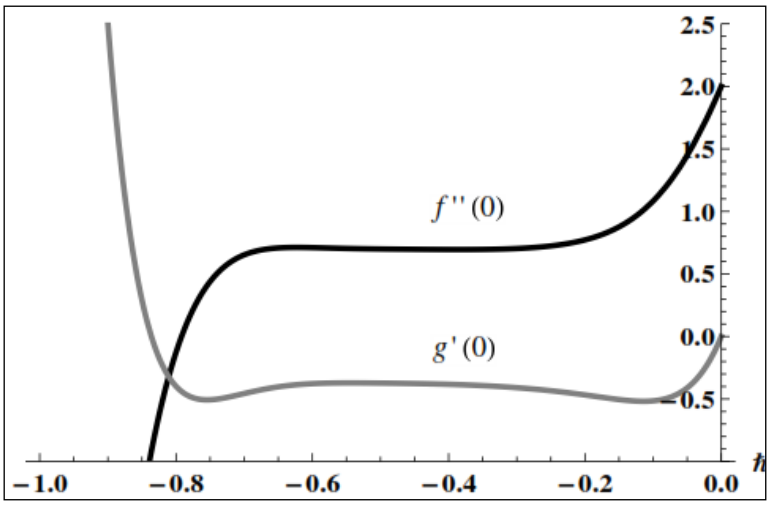


**Figure 4** The $\hbar$-curves of $f''(0)$ and $g'(0)$ obtained by the 10th order approximation of HAM, when $\delta = 1$.

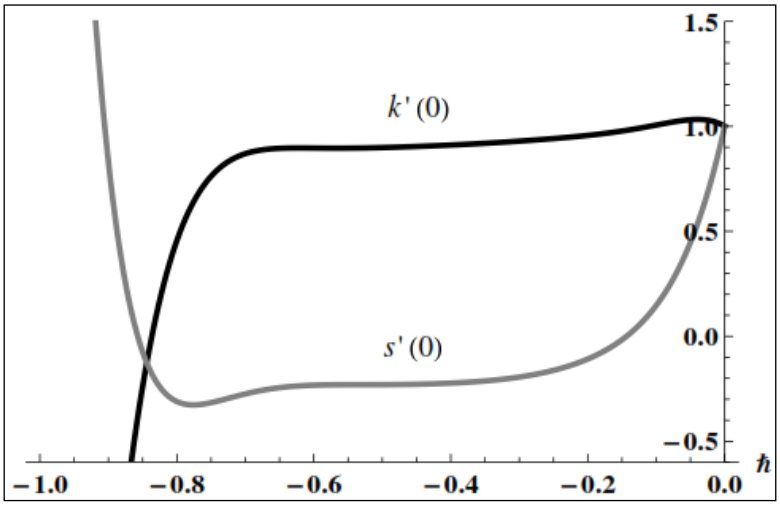


**Figure 5** The $\hbar$-curves of $k'(0)$ and $s'(0)$ obtained by the10th order approximation of HAM, when $\delta = 1$.

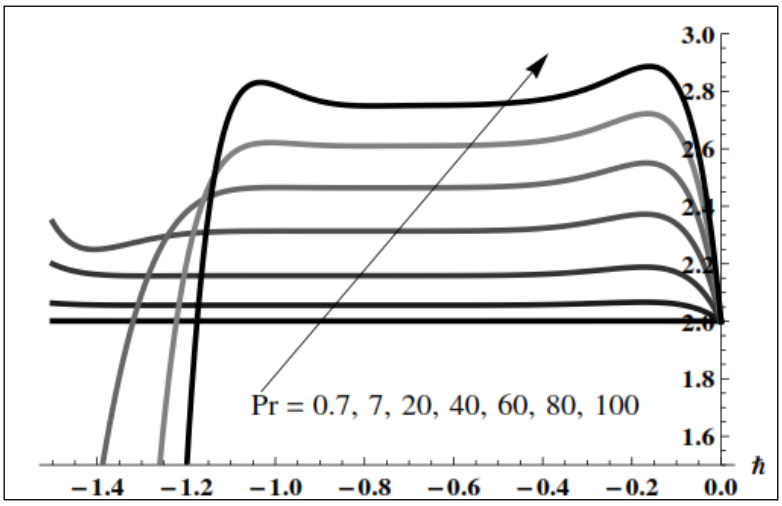


**Figure 6** The $\hbar$-curves of $\theta'(0)$ obtained by the 10th order approximation of HAM at different values of *Pr*, when $\delta = 0.5$.

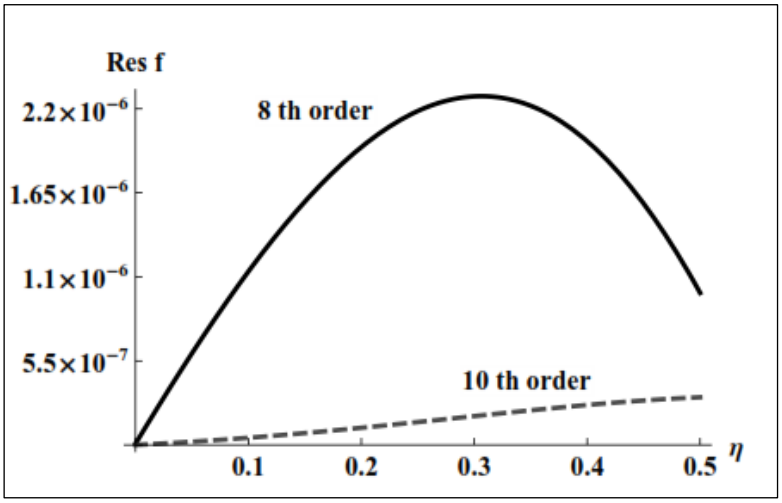


**Figure 7** The absolute residual *f* for $\delta = 0.5$ for different orders of approximation of HAM at optimal values of $\hbar_1$, $\hbar_2$ and $\hbar_3$.

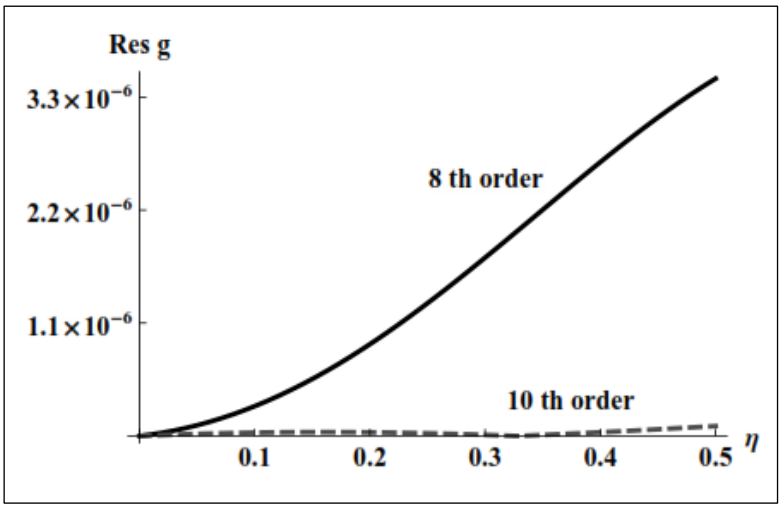


**Figure 8** The absolute residual $g$ for $\delta = 0.5$ for different orders of approximation of HAM at optimal values of $\hbar_1$, $\hbar_2$ and $\hbar_3$.

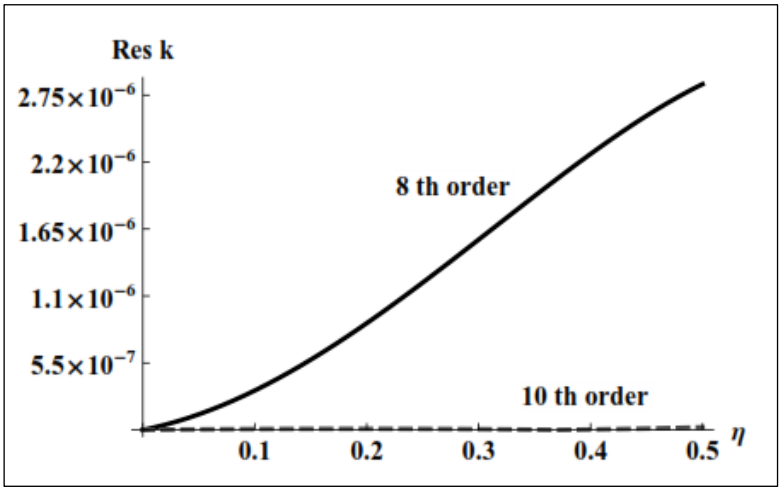


**Figure 9** The absolute residual $k$ for $\delta = 0.5$ for different orders of approximation of HAM at optimal values of $\hbar_1$, $\hbar_2$ and $\hbar_3$.

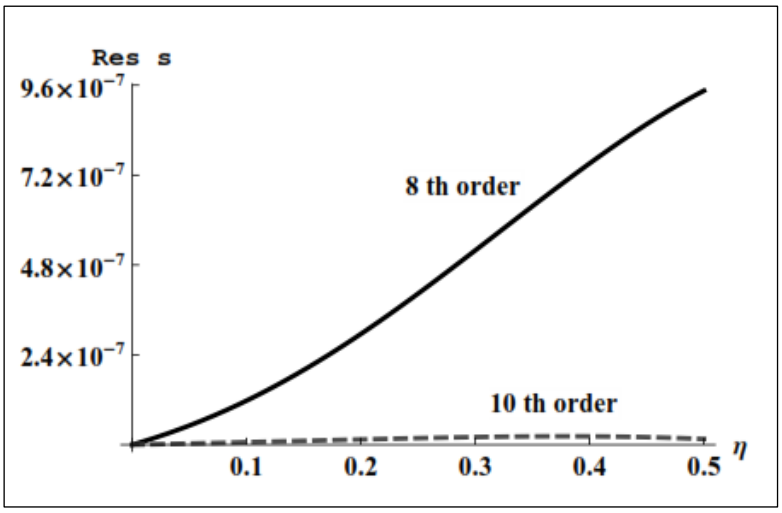


**Figure 10** The absolute residual s for $\delta = 0.5$ for different orders of approximation of HAM at optimal values of $\hbar_1$, $\hbar_2$ and $\hbar_3$.

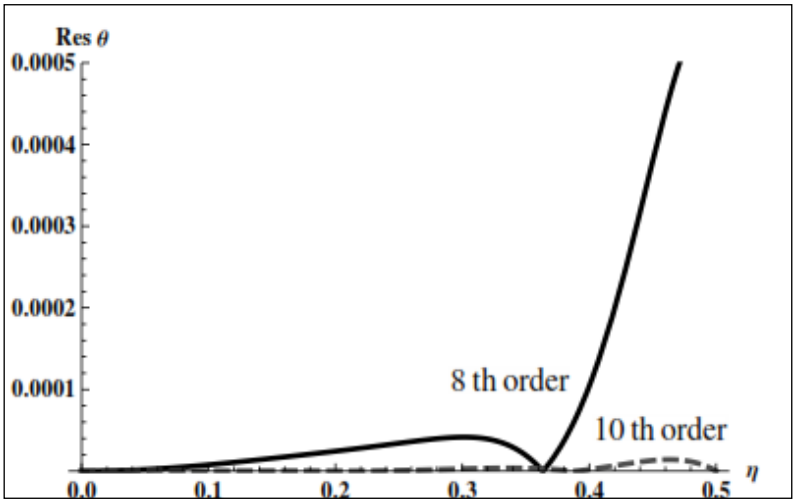


**Figure 11** The absolute residual $\theta$ for $\delta = 0.5$ and Pr = 20 for different orders of approximation of HAM at optimal values of $\hbar_1$, $\hbar_2$ and $\hbar_3$.

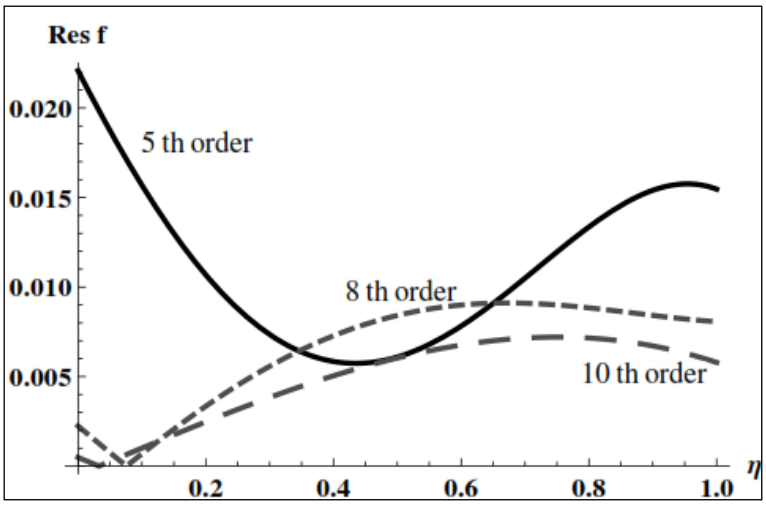


**Figure 12** The absolute residual $f$ for $\delta = 1$ and for different orders of approximation of HAM at optimal values of $\hbar_1$, $\hbar_2$ and $\hbar_3$.

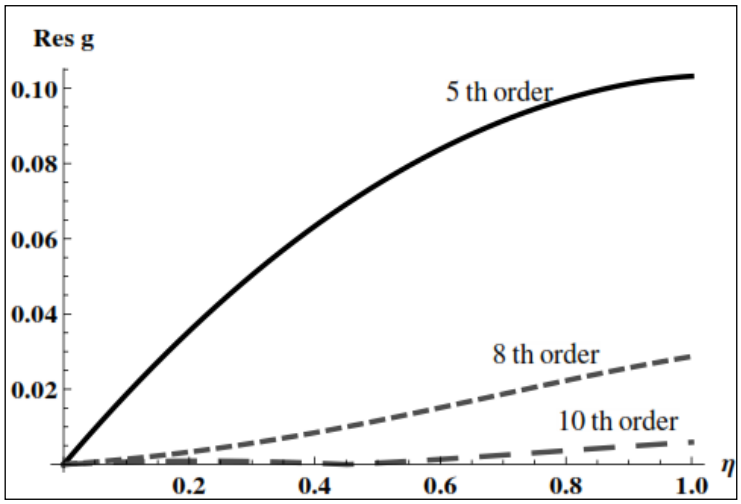


**Figure 13** The absolute residual $g$ for $\delta = 1$ for different orders of approximation of HAM at optimal values of $\hbar_1$, $\hbar_2$ and $\hbar_3$.

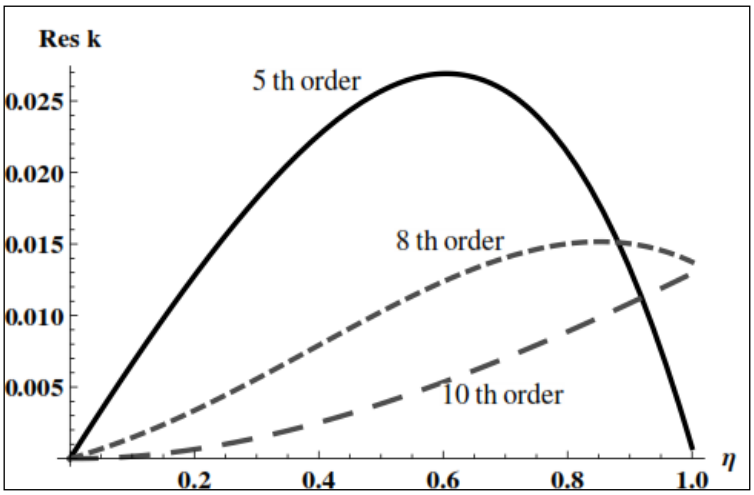


**Figure 14** The absolute residual $k$ for $\delta = 1$ for different orders of approximation of HAM at optimal values of $\hbar_1$, $\hbar_2$ and $\hbar_3$.

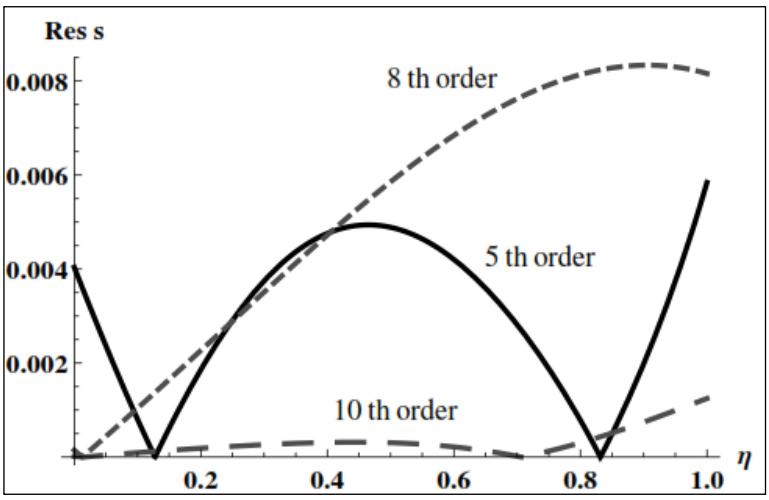


**Figure 15** The absolute residual $s$ for $\delta = 1$ for different orders of approximation of HAM at optimal values of $\hbar_1$, $\hbar_2$ and $\hbar_3$.

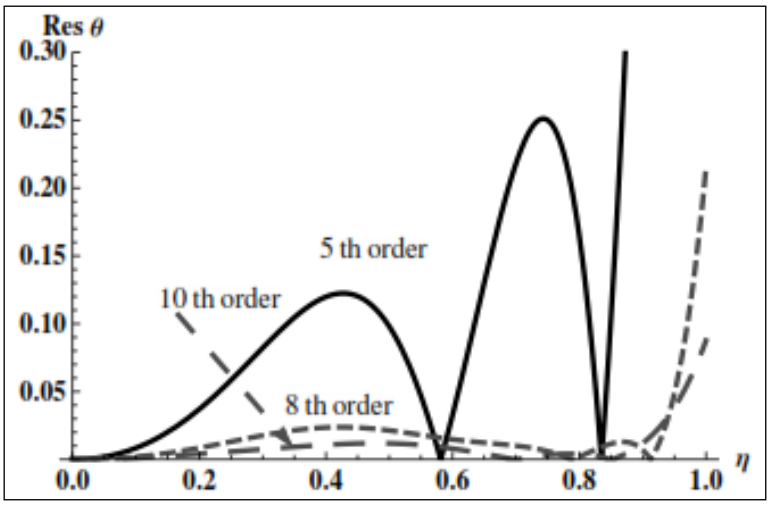


**Figure 16** The absolute residual $\theta$ for $\delta = 1$ and Pr = 20 for different orders of approximation of HAM at optimal values of $\hbar_1$, $\hbar_2$ and $\hbar_3$.

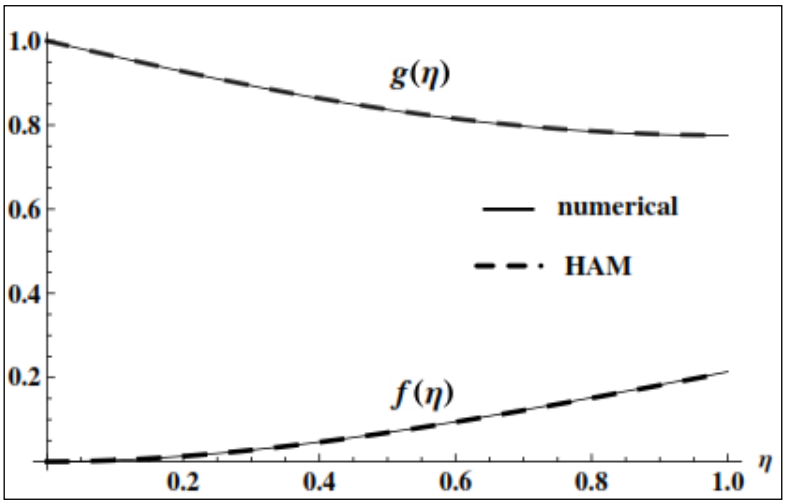


**Figure 17** The normalized radial velocity profiles for the rotating flow obtained by the 10th-order approximation of the HAM for $\delta = 1$ in comparison with the numerical solution, at optimal values of $\hbar_1$, $\hbar_2$ and $\hbar_3$.

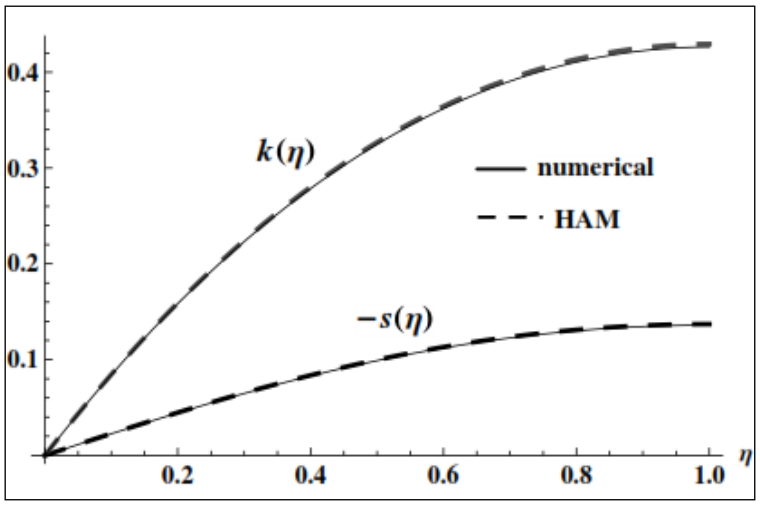


**Figure 18** The normalized velocity profiles for the draining flow $k(\eta)$ and lateral flow $s(\eta)$ obtained by the 10th-order approximation of the HAM for $\delta = 1$ in comparison with the numerical solution, at optimal values of $\hbar_1$, $\hbar_2$ and $\hbar_3$.

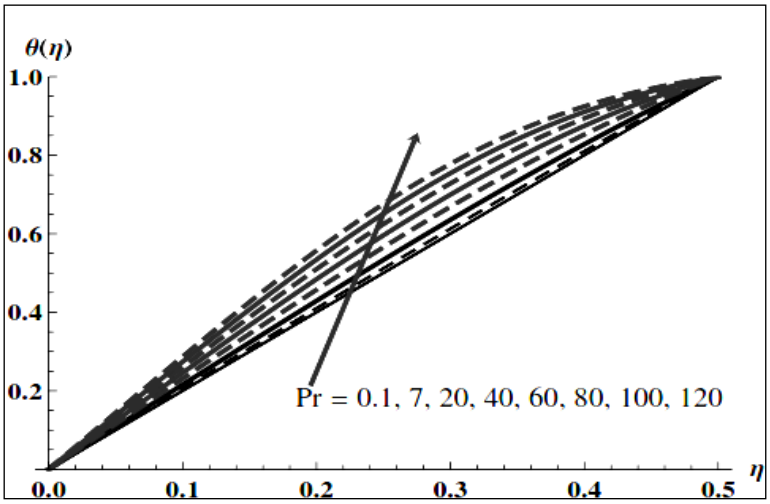


**Figure 19** The normalized temperature profiles $\theta(\eta)$ obtained by the 10th-order approximation of the HAM for different values of the Prandtl number, when $\delta = 0.5$.

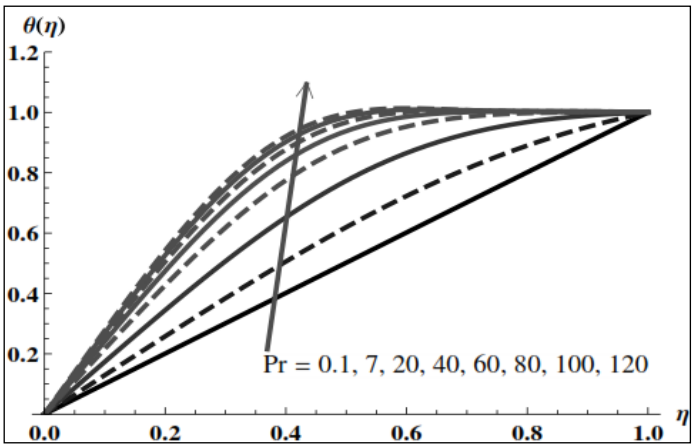


**Figure 20** The normalized temperature profiles $\theta(\eta)$ obtained by the 10th-order approximation of the HAM for different values of the Prandtl number, when $\delta = 1$.

**Table 1** Optimal values of $\hbar_1$ and $\hbar_2$ for different values of $\delta$ at 10th-order approximation.

| $\delta$ | $\hbar_1$ | $\hbar_2$ |
|---|---|---|
| 0.5 | -0.90376 | -1.00479 |
| 1 | -0.53355 | -0.66794 |

**Table 2** Optimal values of $\hbar_3$ for different values of Pr at 10th-order approximation.

| **Pr** | **0.1** | **7** | **20** | **40** | **60** | **80** | **100** | **120** |
|---|---|---|---|---|---|---|---|---|
| $\hbar_3$ at $\delta = 0.5$ | -1.19438 | -0.97365 | -0.93125 | -0.73685 | -0.45190 | -0.45175 | -0.45039 | -0.44353 |
| $\hbar_3$ at $\delta = 1$ | -0.40432 | -0.24331 | -0.23035 | -0.15443 | -0.11201 | -0.08787 | -0.07224 | -0.06129 |

**Table 3** The analytic results of $f(\eta)$ and $g(\eta)$ at different values of $\eta$ compared with the numerical results, when $\delta = 1$ at optimal values of $\hbar_1$ and $\hbar_2$.

| $\eta$ | $f(\eta)$ | | $g(\eta)$ | |
|---|---|---|---|---|
| | **HAM** | **Num** | **HAM** | **Num** |
| 0 | 0.000000 | 0.000000 | 0.000000 | 0.000000 |
| 0.1 | 0.003347 | 0.003364 | 0.003347 | 0.003364 |
| 0.2 | 0.012800 | 0.012825 | 0.012800 | 0.012825 |
| 0.3 | 0.027345 | 0.027490 | 0.027345 | 0.027490 |
| 0.4 | 0.046281 | 0.046535 | 0.046281 | 0.046535 |
| 0.5 | 0.068807 | 0.069195 | 0.068807 | 0.069195 |
| 0.6 | 0.094217 | 0.094763 | 0.094217 | 0.094763 |
| 0.7 | 0.121859 | 0.122580 | 0.121859 | 0.122580 |
| 0.8 | 0.151124 | 0.150320 | 0.151124 | 0.150320 |
| 0.9 | 0.181442 | 0.182545 | 0.181442 | 0.182545 |
| 1 | 0.212274 | 0.213575 | 0.212274 | 0.213575 |

**Table 4** The analytic results of $k(\eta)$ and $-s(\eta)$ at different values of $\eta$ compared with the numerical results, when $\delta = 1$ at optimal values of $\hbar_1$ and $\hbar_2$.

| $\eta$ | $k(\eta)$ | | $-s(\eta)$ | |
|---|---|---|---|---|
| | **HAM** | **Num** | **HAM** | **Num** |
| 0 | 0.000000 | 0.000000 | 0.000000 | 0.000000 |
| 0.1 | 0.084529 | 0.084113 | 0.022742 | 0.022565 |
| 0.2 | 0.159275 | 0.158444 | 0.044681 | 0.044332 |
| 0.3 | 0.224444 | 0.223201 | 0.065152 | 0.064642 |
| 0.4 | 0.280230 | 0.278584 | 0.083628 | 0.082971 |
| 0.5 | 0.326824 | 0.324796 | 0.099702 | 0.098919 |
| 0.6 | 0.364424 | 0.362047 | 0.113081 | 0.112194 |
| 0.7 | 0.393240 | 0.390561 | 0.123568 | 0.122603 |
| 0.8 | 0.413499 | 0.410583 | 0.131057 | 0.130038 |
| 0.9 | 0.425452 | 0.422380 | 0.135515 | 0.134467 |
| 1 | 0.429372 | 0.426243 | 0.136982 | 0.135925 |

## Conclusions

In this work, the OHAM has been successfully implemented to develop analytical solutions of the system of nonlinear ordinary differential equations derived from similarity transformation of the steady three-dimensional problem of fluid deposition on an inclined rotating disk. The convergence analyses show that the optimal homotopy analysis method gives accurate results for a large thickness of the fluid film. For a fixed value of the film thickness, the OHAM is valid for large Prandtl numbers. The effects of thickness of the fluid film on the profiles of temperature, radial velocity for the rotating flow, velocity for the draining flow and lateral flow illustrated with graphs. The effect of Prandtl numbers on the temperature profile was illustrated with graphs. When compared with the numerical results, the present results are found to be highly accurate and consistent with the numerical results pertaining to the same problem. The use of the concept of averaged residual recently introduced by Liao [29] greatly improves the rate of the convergence of the analytical solution by allowing the determination of the optimal auxiliary parameter. Consequently, the present method of the OHAM is successful for the nonlinear problem of three-dimensional steady flow of condensation film on an inclined rotating disk and verifies that the present method is a useful tool for highly nonlinear problems in science and engineering.

## References

[1] AH Nayfeh. *Introduction to Perturbation Techniques*. John Wiley & Sons, 1979, p. 1-533.
[2] RH Rand and D Armbruster. *Perturbation Methods, Bifurcation Theory and Computer Algebraic*. Springer-Verlag, New York, 1987, p. 1-243.
[3] SJ Liao. 1992, The proposed homotopy analysis technique for the solution of nonlinear problems. Ph. D. Thesis, Shanghai Jiao Tong University.
[4] M Sajid, T Hayat and S Asghar. Comparison between the HAM and HPM solutions of thin film flows of non-Newtonian fluids on a moving belt. *Nonlinear Dyn*. 2007; **50**, 27-35.
[5] SJ Liao and Y Tan. A general approach to obtain series solutions of nonlinear differential equations. *Stud. Appl. Math.* 2007; **119**, 297-355.
[6] SJ Liao. On the analytic solution of magneto hydrodynamic flows of non-Newtonian fluids over a stretching sheet. *J. Fluid Mech*. 2003; **488**, 189-212.
[7] T Hayat, M Mustafa and S Asghar. Unsteady flow with heat and mass transfer of a third grade fluid over a stretching surface in the presence of chemical reaction. *Nonlinear Anal. Real World Appl.* 2010; **11**, 3186-97.

[8] T Hayat, M Qasim and Z Abbas. Homotopy solution for the unsteady three-dimensional MHD flow and mass transfer in a porous space. *Comm. Nonlinear Sci. Numer. Simulat.* 2010; **15**, 2375-87.
[9] MM Rashidi, G Domairry and S Dinarvand. The homotopy analysis method for explicit analytical solutions of Jaulent-Miodek equations. *Num. Meth. Part. Diff. Eqs*. 2009; **25**, 430-9.
[10] MM Rashidi, G Domairry and S Dinarvand. Approximate solutions for the Burgers' and regularized long wave equations by means of the homotopy analysis method. *Comm. Nonlinear Sci. Numer. Simulat.* 2009; **14**, 708-17.
[11] S Dinarvand and MM Rashidi. A reliable treatment of homotopy analysis method for two dimensional viscous flow in a rectangular domain bounded by two moving porous walls. *Nonlinear Anal. Real World Appl.* 2010; **11**, 1502-12.
[12] S Abbasbandy. The application of homotopy analysis method to nonlinear equations arising in heat transfer. *Phys. Lett. A* 2006; **360**, 109-13.
[13] HN Hassan and MA El-Tawil. An efficient analytic approach for solving two-point nonlinear boundary value problems by homotopy analysis method. *Math. Meth. Appl. Sci.* 2011; **34**, 977-89.
[14] HN Hassan and MA El-Tawil. A new technique for using homotopy analysis method for solving high-order nonlinear differential equations. *Math. Meth. Appl. Sci.* 2011; **34**, 728-42.
[15] S Abbasbandy and E Shivanian. Prediction of multiplicity of solutions of nonlinear boundary value problems: novel application of homotopy analysis method. *Comm. Nonlinear Sci. Numer. Simulat.* 2010; **15**, 3830-46.
[16] HN Hassan and MA El-Tawil. Solving cubic and coupled nonlinear Schrödinger equations using the homotopy analysis method. *Int. J. Appl. Math. Mech.* 2011; **7**, 41-64.
[17] MM Rashidi, T Hayat, E Erfani, SAM Pour and AA Hendi. Simultaneous effects of partial slip and thermal-diffusion and diffusion-thermo on steady MHD convective flow due to a rotating disk. *Comm. Nonlinear Sci. Numer. Simulat.* 2011; **16**, 4303-17.
[18] SH Nourbakhsh, AAP Zanoosi and AR Shateri. Analytical solution for off-centered stagnation flow towards a rotating disc problem by homotopy analysis method with two auxiliary parameters. *Comm. Nonlinear Sci. Numer. Simulat*. 2011; **16**, 2772-87.
[19] EM Sparrow and JL Gregg. A theory of rotating condensation. *Trans. ASME Series C* 1959; **81**, 113-20.
[20] TV Karman. Uber laminare und turbulente reibung. *Zeitschrift fur Angewandte Mathematik und Mechanik* 1921; **1**, 233-52.
[21] PM Beckett, PC Hudson and G Poots. Laminar film condensation due to a rotating disk. *J. Eng. Math.* 1973; **7**, 63-73.
[22] SP Chary and PK Sarma. Condensation on a rotating disk with constant axial suction. *J. Heat Tran.* 1976; **98**, 682-4.
[23] KF Jensen, EO Einset and DI Fotiadis. Flow phenomena in chemical vapor deposition of thin films. *Annu. Rev. Fluid Mech.* 1991; **23**, 197-232.
[24] CY Wang. Condensation film on an inclined rotating disk. *Appl. Math. Model.* 2007; **31**, 1582-93.
[25] MM Rashidi and SAM Pour. Analytic solution of steady three-dimensional problem of condensation film on inclined rotating disk by differential transform method. *Math. Probl. Eng.* 2010; **2010**, 613230.
[26] A Arikoglu, G Komurgoz and I Ozkol. Effect of slip on the entropy generation from a single rotating disk. *J. Fluids Eng.* 2008; **130**, 1012021-9.
[27] A Arikoglu and I Ozkol. On the MHD and slip flow over a rotating disk with heat transfer. *Int. J. Numer. Meth. Heat Fluid Flow* 2006; **16**, 172-84.
[28] SJ Liao. *Beyond Perturbation: An Introduction to Homotopy Analysis Method*. Boca Raton, Chapman Hall/CRC Press, 2003.
[29] SJ Liao. An optimal homotopy-analysis approach for strongly nonlinear differential equations. *Comm. Nonlinear Sci. Numer. Simulat.* 2010; **15**, 2003-16.